



Published in final edited form as:

Life Sci. 2021 December 01; 286: 120067. doi:10.1016/j.lfs.2021.120067.

Enhanced pro-BDNF-p75NTR pathway activity in denervated skeletal muscle

Katherine Aby, Ryan Antony, Mary Eichholz, Rekha Srinivasan, Yifan Li

Division of Basic Biomedical Sciences, Sanford School of Medicine, University of South Dakota, Vermillion, SD 57069, USA

Abstract

Aims: Brain derived neurotrophic factor (BDNF) and the related receptors TrkB and p75NTR are expressed in skeletal muscle, yet their functions remain to be fully understood. Skeletal muscle denervation, which occurs in spinal injury, peripheral neuropathies, and aging, negatively affects muscle mass and function. In this study, we wanted to understand the role of BDNF, TrkB, and p75NTR in denervation-induced adverse effects on skeletal muscle.

Main methods: Mice with unilateral sciatic denervation were used. Protein levels of pro- and mature BDNF, TrkB, p75NTR, activations of their downstream signaling pathways, and inflammation in the control and denervated muscle were measured with Western blot and tissue staining. Treatment with a p75NTR inhibitor and BDNF skeletal muscle specific knockout in mice were used to examine the role of p75NTR and pro-BDNF.

Key findings: In denervated muscle, pro-BDNF and p75NTR were significantly upregulated, and JNK and NF- κ B, two major downstream signaling pathways of p75NTR, were activated, along with muscle atrophy and inflammation. Inhibition of p75NTR using LM11A-31 significantly reduced JNK activation and inflammatory cytokines in the denervated muscle. Moreover, skeletal muscle specific knockout of BDNF reduced pro-BDNF level, JNK activation and inflammation in the denervated muscle.

Significance: These results reveal for the first time that the upregulation of pro-BDNF and activation of p75NTR pathway are involved in denervation-induced inflammation in skeletal muscle. The results suggest that inhibition of pro-BDNF-p75NTR pathway can be a new target to treat skeletal muscle inflammation.

Corresponding author: Yifan Li, PhD, Professor of Physiology, Division of Basic Biomedical Sciences, Sanford School of Medicine, University of South Dakota, 414 East Clark Street, Vermillion, SD 57069, Tel. 605 658-6319, yifan.li@usd.edu.
Author contribution

Katherine Aby: Methodology, investigation, visualization, formal analysis, writing-original draft, writing-review and editing.

Ryan Antony: Methodology, investigation

Mary Eichholz: Investigation

Rekha Srinivasan: Investigation

Yifan Li: Conceptualization, methodology, formal analysis, investigation, writing-original, writing-review and editing, and project administration.

Publisher's Disclaimer: This is a PDF file of an unedited manuscript that has been accepted for publication. As a service to our customers we are providing this early version of the manuscript. The manuscript will undergo copyediting, typesetting, and review of the resulting proof before it is published in its final form. Please note that during the production process errors may be discovered which could affect the content, and all legal disclaimers that apply to the journal pertain.

Conflict of interest

The authors declare no conflict of interest related to this study.

Keywords

BDNF; p75NTR; myokine; denervation; inflammation

Introduction

Skeletal muscle is the largest tissue in the body, accounting for approximately 40% of body mass. Skeletal muscle fibers are highly heterogenic and highly plastic tissue in terms of contractile dynamics and metabolism[1]. Skeletal muscle mass, function, and metabolism alter in response to changes in workload, nutrient supply, and nerve control. For example, muscle atrophy can be caused by disuse and unloading, insufficient nutrient supply, aging, denervation, and various chronic illnesses[2, 3]. Particularly, innervation is critical for maintenance of skeletal muscle mass and function. Muscle denervation, which may occur in spinal injury, nerve damage, peripheral neuropathies, and aging, leads to muscle inflammation, oxidative stress, and atrophy. Despite extensive research, the mechanisms and factors involved in denervation-induced muscle atrophy remain to be fully understood.

Inflammation plays a major pathogenic role in skeletal muscle injury and atrophy in various conditions, including sepsis[4], aging[5], and denervation[6]. Pro-inflammatory cytokines such as IL-6[7] and TNF α [7] are well documented to cause muscle atrophy. Inflammatory cytokines increase protein degradation via ubiquitin-proteasomal pathway[8]. In addition, inflammation also inhibits IGF-Akt pathway and thus reduces protein synthesis[9]. Emerging studies show that various treatments alleviate denervation-induced muscle atrophy through anti-inflammatory mechanisms[7, 10, 11]. Infiltration of macrophages and neutrophils into skeletal muscle are considered as the major sources of inflammatory cytokines in muscle injury[12]. The infiltration of macrophages and neutrophils and their functional roles in denervated skeletal muscle remain to be fully understood.

Brain derived neurotrophic factor (BDNF), originally discovered in the brain[13], belongs to the neurotrophic factor family and plays a critical role in neuron growth, neuronal network development, and synaptic plasticity and function[14–17]. Recently, BDNF has been identified as a myokine that is expressed and released from skeletal muscle[18]. It is evident that muscle-derived BDNF is involved in regulation of metabolism and energy homeostasis[18–20], and muscle regeneration[21]. In neurons, BDNF can be released as mature BDNF as well as pro-BDNF[22]. While mature BDNF binds and stimulates TrkB receptors, pro-BDNF binds and stimulates p75NTR receptors to activate different downstream signaling pathways and elicit different functional effects in the nervous system[22, 23]. Currently, the studies on myokine BDNF are primarily focused on mature BDNF and the TrkB pathway. The expression and function of pro-BDNF and p75NTR pathway in skeletal muscle remain unknown. In this study, we reported that denervation upregulated proBDNF and activated p75NTR pathway, which mediates muscle inflammation.

Method

Unilateral sciatic denervation

All experimental protocols and use of animals in this study were reviewed and approved by the University of South Dakota Institutional Animal Care and Use Committee (IACUC) and followed the NIH guideline of animal use in research. Male and female C57/B6 mice between the ages of 3 to 4 months were chosen at random for sciatic denervation surgery. Under anesthesia with isoflurane gas, the hair covering the right hind limb joint was removed using Nair and the skin was disinfected. An approximately 1cm lengthwise incision was made in the skin in the area where the fur was removed. The connective tissue just over the right hip was snipped to reveal the sciatic nerve trunk. Using forceps, the sciatic nerve was grasped, and a portion snipped to prevent regrowth or reconnection of the neural tissue. The incision was closed and sealed with surgical glue (Veterinary tissue adhesive TA5). Buprenorphine SR (1mg/kg) was given subcutaneously. The left hind limb without surgery and denervation was used as the control. Mice were allowed to recover from anesthesia in a warmed cage and then returned to the home cage.

Treatment with LM11A-31

Upon returning to their home cages after sciatic denervation, one group of mice were given standard drinking water *ad libitum* as a control, while a treatment group was given water containing LM11A-31 (Cayman Chemical, reconstituted in DMSO), a small molecule modulator that inhibits the binding of pro-BDNF to p75NTR, at a rate of 75mg/kg/day for one week. The dose of LM11A-31 was chosen according to the previous reports[24, 25].

Skeletal muscle specific knockout of BDNF

BDNF flox/flox mice[26] were purchased from Jackson Laboratory (catalog No. 004339). These mice were crossed with mice expressing cre recombinase driven by the skeletal muscle-specific myosin light chain promoter (Jackson Laboratory, 024713) to generate skeletal muscle specific knockout of BDNF. The resulting strain was backcrossed for at least 5 generations. Mice with genotype of homozygous flox/flox/cre (skeletal muscle BDNF knockout, smKO) or with flox/flox (WT control) were used in this study.

Tissue dissection

At the end of the denervation or treatment periods, mice were anesthetized using isoflurane, skin of the hind limbs was removed and the soleus, extensor digitorum longus (EDL), tibialis anterior (TA), and plantaris in both denervation and contralateral sides were dissected off and snap frozen. For tissue staining, the dissected muscles were coated with optimal cutting temperature (OCT) compound and snap frozen in 2-methylbutane (isopentane) that was prechilled with dry ice. For Western blot, dissected tissues were quickly frozen on dry ice. All tissues were stored at -75°C until use.

Homogenization and western blot sample preparation

The soleus and EDL were homogenized using plastic pestles (Fisher) in RIPA buffer containing 1:100 protease and phosphatase inhibitor cocktails (Fisher), 0.2% SDS, and

1 μ M of MG132. After homogenization, samples were left on ice for 30 minutes before centrifugation at 10,000 \times *g* for 10 minutes. The supernatant of homogenates was collected. The protein concentration in the supernatants was determined using a BCA protein assay (ThermoFisher) and normalized, and equal amount of proteins was mixed with loading buffer for Western blot, as described previously[27, 28].

Western blot

Tissue or cell samples were subjected to electrophoresis on 11–16% SDS-PAGE gels at 70V for 15 minutes, followed by 100V for approximately 2.5 hours. The separated proteins were transferred onto 0.45 μ m or 0.22 μ m nitrocellulose membrane (Nitrobind pure nitrocellulose membrane, Santa Cruz) at 350mA for 2 hours. Membranes were fixed with 50% methanol for 30 minutes at 4°C followed by 30 minutes at 37°C. Membranes were then blocked using 10mL of 3% milk (Chem Cruz Blotto low-fat dry milk) made with PBST at room temperature for 1 hour with rocking. Membranes were cut and placed in primary antibodies diluted in PBST containing 0.5% BSA. Primary antibodies used were p75NTR (1:1000 Cell Signaling Technologies, 8238S), TrkB (1:1000, ProteinTech, 13129–1-AP), pro-BDNF (1:500 Santa Cruz, sc-6551), BDNF (1:1000 Abcam, ab108319), Furin (1:1000 ABclonal, A7445), p-JNK (1:1000 Cell Signaling Technologies, 9255S), p-I κ B (1:1000 Cell Signaling Technologies, 2859S), p-ERK (1:1000 Cell Signaling Technologies, 57265S), p-AKT T308 (1:1000 Cell Signaling Technologies, 13038S), TNF α (1:500 Santa Cruz, sc-8301), IL-6 (1:500 Santa Cruz, sc-5731), TGF- β (1:1000 Biologend, 141402), IL-1 β (1:1000 Biologend, 503502). The membranes were incubated at 4°C overnight (approximately 16 hours) on a rocker. Primary antibodies were then removed, and membranes were washed with PBST in 3 washes of 5 minutes each. Following washes, membranes were incubated in 3mL of fluorescence conjugated secondary antibodies (1:10,000 dilution in PBST with 0.02% sodium azide) on a rocker for 1 hour at room temperature. Membranes were then washed in two 5-minute washes with PBST and one 5-minute wash with PBS. For loading control, total proteins in the membrane were stained with a total protein stain reagent (Revert 700, LI-COR, 926–11011). A clear nonspecific protein band was chosen as loading control for Western blot quantification. Membranes were imaged using the LI-COR scanner and Image Studio software.

Immunofluorescent staining

TA muscles were used for tissue staining. Once harvested and snap frozen, the muscle was covered in OTC. Sections were cut using a cryostat (Leica) set at 10 μ m and mounted to charged slides. Slides were dried for 30 minutes and OTC was removed. Sections were circled with a hydrophobic pen. The sections were incubated in blocking solution (PBS containing 1% BSA and 15% goat serum) in a moisture box for one hour at room temperature. Blocking solution was then aspirated and sections were incubated in diluted primary antibodies (1:100 to 1:25 in PBS containing 1% BSA) in the moisture box overnight at 4°C. The primary antibodies include p75NTR (1:100, Cell Signaling Technologies, 8238S), CD68 (1:100, Biologend, 137020), or dystrophin (1:100, Abcam, 15277). Slides were then washed in PBS 3 times for 5 minutes each. Fluorescence conjugated secondary antibodies were diluted (1:500 in PBS containing 1% BSA) and sections were incubated in the diluted secondary antibody for 1 hour at room temperature. Following three washes of

5 minutes each with PBS, slides were dried and then mounted with fluormount solution (Southern biotech fluoromount-G). Images were taken using a fluorescent microscope (Olympus).

Data analysis and statistics

Western blot gel images and muscle dystrophin staining images were quantified using Image J. Statistical analysis was performed using Excel for t-tests and ANOVA analyses, and SAS studio for Chi squared analysis. Quantified data were presented as mean \pm standard deviation. P values less than 0.05 were considered as statistically significant.

Results

1, Upregulation of pro-BDNF and p75NTR in denervated skeletal muscle

Using mice with unilateral sciatic denervation for one week, we first compared the protein levels of mature BDNF and pro-BDNF in soleus from the denervated and innervated side of hindlimbs. We found that the pro-BDNF protein level was significantly upregulated in the denervated muscle. The changes in mature BDNF varied with a trend of reduction in the denervated muscle (Fig. 1A). Moreover, the protein level of a major BDNF convertase furin[22, 29] was significantly downregulated in denervated muscle (Fig. 1B), suggesting a potential cause of the upregulation of pro-BDNF.

We then compared the protein levels of TrkB, the receptor of mature BDNF, and p75NTR, the receptor of pro-BDNF, and found that full length TrkB was significantly downregulated whereas p75NTR was significantly upregulated in denervated muscle (Fig. 1C and D). The upregulations of pro-BDNF and its receptor p75NTR indicate the potential enhanced activity of this pathway in the denervated muscle.

2, Alterations of downstream signaling pathways in denervated muscle

TrkB and p75NTR induce different cellular responses and processes via different downstream signaling pathways. Upon stimulation, TrkB activates ERK1/2 pathway and Akt pathway, whereas p75NTR activates JNK and NF-kB pathways[30]. We then measured the activation of these pathways. As shown in Fig. 2, the phosphorylation of JNK and I κ B, as well as NF-kB2 active form p52[31] were significantly increased in the denervated muscle (Fig. 2A and B). In contrast, the phosphorylation of Akt (T308) and ERK were significantly reduced in the denervated muscle (Fig. 2C and D). This data confirms the enhanced activation of p75NTR pathway and reduced activation of TrkB pathway in denervated muscle.

3, Muscle atrophy and inflammation in denervated muscle

JNK and NF-kB pathways are known for their roles in inflammation and muscle atrophy. As expected, denervated muscle developed muscle atrophy (Fig. 3A) and increased proinflammatory cytokines (Fig. 3B to E). Moreover, the macrophage infiltration was increased in denervated muscle (Fig. 3F). The enhanced p75NTR activation and its downstream pathways may contribute to the muscle inflammation and atrophy in the denervated muscle.

4, Blockage of p75NTR attenuated JNK pathway activation in denervated muscle

To determine whether p75NTR is involved in the activation of JNK and upregulation of inflammatory cytokines in the denervated muscle, mice were treated with a small molecule p75NTR modulator LM11A-31 that blocks pro-BDNF from binding to p75NTR. As shown in Fig. 4, the treatment with LM11A-31 significantly attenuated phosphorylation of JNK in denervated muscle (Fig. 4A and D), suggesting that p75NTR mediated the activation of JNK pathway. The treatment with LM11A-31 did not alter the upregulation of p75NTR nor the downregulation of TrkB (Fig. 4B and C), suggesting that p75NTR stimulation may not affect the expressions of these receptors.

5, Blockage of p75NTR mitigated inflammation in denervated muscle

The treatment with LM11A-31 significantly attenuated the upregulation of pro-inflammatory cytokine IL-6 and TGF β in the denervated muscle (Fig. 5A to C), suggesting p75NTR activation is involved in denervation-induced inflammation. Interestingly, the upregulation of another pro-inflammatory cytokine IL-1 β in the denervated muscle was unaffected by the treatment (Fig. 5D). Additionally, macrophage infiltration in denervated muscle also did not attenuated by the treatment (Fig. 5F). These data suggest that p75NTR regulation of inflammation is target specific. Muscle atrophy was assessed by the distribution of muscle fiber sizes measured by cross sectional area. There was not a statistically significant difference between denervated muscle treated with LM11A-31 and the untreated denervated muscle (Fig. 5E).

6, BDNF muscle knockout reduced muscle inflammation in denervated muscle

To determine whether the skeletal muscle derived pro-BDNF plays a role in stimulation of p75NTR in muscle, we used mice with skeletal muscle specific knockout (smKO) of BDNF, which exhibited a reduction of pro-BDNF protein level (Fig. 6A). While the upregulation of p75NTR and downregulation of TrkB in the denervated muscle were unaffected in WT and BDNF smKO mice (data were not shown), the phosphorylation of JNK was attenuated in BDNF smKO muscle (Fig. 6A and B), suggesting that myokine pro-BDNF is involved in stimulation and activation of p75NTR-JNK pathway. Moreover, BDNF smKO mitigated increased IL-6 (Fig. 6A and C) and macrophage infiltration (Fig. 6D). There was no significant change in muscle atrophy of the denervated muscle in BDNF smKO mice as compared to WT, though (Fig. 6E).

Discussion

BDNF as a skeletal muscle derived myokine has been well documented[9, 10]. Myokine BDNF regulates muscle metabolism[19, 20, 32], satellite cell differentiation and muscle regeneration[21, 33], and muscle fiber specificity[34]. These studies were mainly focused on the mature BDNF-TrkB pathway. In neurons, pro-BDNF can also be released and elicits distinct functions by binding and stimulating p75NTR[22, 35, 36]. To date, however, the expression, regulation, and function of the pro-BDNF-p75NTR pathway in skeletal muscle remain poorly understood. The present study for the first time shows that in denervated skeletal muscle pro-BDNF and its receptor p75NTR were both upregulated. These upregulations are accompanied with the increased activation of JNK and NF- κ B pathways,

two major p75NTR downstream signaling pathways, and increased inflammatory cytokines, such as IL-6, in the denervated muscle. Importantly, the treatment with LM11A-31, the small molecule modulator that blocks pro neurotrophins, including pro-BDNF, from binding to p75NTR, significantly attenuated JNK activation and IL-6 levels in the denervated muscle. Together, these results indicate that enhanced pro-BDNF-p75NTR pathway activity may at least partially contribute to the adverse changes such as inflammation in the denervated muscle. Targeting pro-BDNF-p75NTR pathway could be a novel strategy for prevention and mitigation of denervation-induced myopathy.

In the nervous system, pro-BDNF and mature BDNF exhibit distinct, even opposite functions. For example, in neurons, mature BDNF promotes long-term potentiation (LTP) [37] whereas pro-BDNF enhances long-term depression (LTD)[38]. While pro-BDNF causes neuron apoptosis, mature BDNF is anti-apoptotic. These opposite effects are critical for appropriate development and function of neuronal network[39, 40]. The unbalanced enhancement of pro-BDNF-p75NTR activity is involved in neuron injury and therefore is a potential therapeutic target for various diseases, such as neurodegenerative diseases[40]. The skeletal muscle derived pro-BDNF and mature BDNF may also elicit distinct effects through p75NTR and TrkB respectively to regulate muscle development, metabolism, and function, which remain to be fully understood. As revealed by our data, the upregulation of pro-BDNF and p75NTR with downregulation of TrkB in denervated muscle represent a case of imbalance between the pro-BDNF-p75NTR pathway and mature BDNF-TrkB pathway. Our results suggest that this imbalance at least contributes to the inflammation in the denervated muscle, because blocking p75NTR attenuated upregulation of inflammatory cytokine IL-6 and TGF β . Interestingly, the upregulation of IL-1 β was unaffected by the treatment, suggesting that p75NTR pathway may regulate inflammation in a cytokine specific manner.

In addition to p75NTR, the upregulation of pro-BDNF may also be a potential therapeutic target. Our data show that skeletal muscle specific knockout of BDNF attenuated upregulation of pro-BDNF and reduced inflammation, further suggesting the detrimental role of pro-BDNF. Pro-BDNF is cleaved to mature BDNF by certain proteases (convertases). Furin, for example, is the major BDNF convertase in the trans Golgi network in neurons[41, 42]. Functions of furin in skeletal muscle have not been studied. Our data show that furin was downregulated in denervated muscle, along with the upregulation of pro-BDNF. This suggests that furin also plays a major role in BDNF cleavage in skeletal muscle and downregulation of furin leads to the upregulation of pro-BDNF in denervated muscle. The cause of the downregulation of furin in denervated muscle needs to be further investigated.

Secreted pro-BDNF can be cleaved to mature BDNF extracellularly by tissue plasmin activator (tPA) and other proteases[37]. The interesting and important questions that have not been examined in this study are whether the extracellular cleavage of pro-BDNF is also reduced in denervated muscle, and whether enhancement of the pro-BDNF cleavage by treatment with proteases such as tPA can mitigate denervation-induced adverse changes in muscles. In addition, TrkB mediates anti-apoptotic and anti-inflammatory effects[43], therefore, downregulation of TrkB may also contribute to the inflammation in the denervated

muscle. The cause of TrkB downregulation and whether stimulation of TrkB can mitigate the denervation-induced adverse changes in muscle would be important for the future study.

Disappointingly, in this study, the treatment with LM11A-31 for one week did not ameliorate denervation-induced muscle atrophy. It would be necessary to examine the effect of longer course of denervation and treatment. In addition, denervation-induced muscle atrophy involves multiple factors and mechanisms, including increased ubiquitination and proteasome-mediated protein degradation, inhibition of protein synthesis, inflammation, and impaired mitochondrial function[2, 44]. We did not observe significant changes in Murf1 or atrogin 1, the major E3 ligases involved in muscle atrophy, or in major mitochondrial markers (data not shown). It would be interesting and necessary to further examine the roles of altered pro-BDNF-p75NTR and mature BDNF-TrkB activities in various mechanisms of muscle atrophy in the future studies.

Supplementary Material

Refer to Web version on PubMed Central for supplementary material.

Acknowledgement

The authors wish to thank Dr. Lisa McFadden and Jaysri Butler for their assistance with statistical analysis and Jessica Freeling for her assistance with animal experiments.

This study was supported by NIH grant 1R01HL147105.

Reference

1. Schiaffino S and Reggiani C, Fiber types in mammalian skeletal muscles. *Physiol Rev*, 2011. 91(4): p. 1447–531. [PubMed: 22013216]
2. Dutt V, et al. , Skeletal muscle atrophy: Potential therapeutic agents and their mechanisms of action. *Pharmacol Res*, 2015. 99: p. 86–100. [PubMed: 26048279]
3. Palus S, von Haehling S, and Springer J, Muscle wasting: an overview of recent developments in basic research. *Int J Cardiol*, 2014. 176(3): p. 640–4. [PubMed: 25205489]
4. Lang CH, et al. , Sepsis and inflammatory insults downregulate IGFBP-5, but not IGFBP-4, in skeletal muscle via a TNF-dependent mechanism. *Am J Physiol Regul Integr Comp Physiol*, 2006. 290(4): p. R963–72. [PubMed: 16339387]
5. Degens H and Alway SE, Control of muscle size during disuse, disease, and aging. *Int J Sports Med*, 2006. 27(2): p. 94–9. [PubMed: 16475053]
6. Shen Y, et al. , Microarray Analysis of Gene Expression Provides New Insights Into Denervation-Induced Skeletal Muscle Atrophy. *Front Physiol*, 2019. 10: p. 1298. [PubMed: 31681010]
7. Huang Z, et al. , Inhibition of IL-6/JAK/STAT3 pathway rescues denervation-induced skeletal muscle atrophy. *Ann Transl Med*, 2020. 8(24): p. 1681. [PubMed: 33490193]
8. Li YP, et al. , TNF-alpha acts via p38 MAPK to stimulate expression of the ubiquitin ligase atrogin1/MAFbx in skeletal muscle. *FASEB J*, 2005. 19(3): p. 362–70. [PubMed: 15746179]
9. Crossland H, et al. , The impact of immobilisation and inflammation on the regulation of muscle mass and insulin resistance: different routes to similar end-points. *J Physiol*, 2019. 597(5): p. 1259–1270. [PubMed: 29968251]
10. Wu C, et al. , Salidroside Attenuates Denervation-Induced Skeletal Muscle Atrophy Through Negative Regulation of Pro-inflammatory Cytokine. *Front Physiol*, 2019. 10: p. 665. [PubMed: 31293430]
11. Choi WH, et al. , Apigenin inhibits sciatic nerve denervation-induced muscle atrophy. *Muscle Nerve*, 2018. 58(2): p. 314–318. [PubMed: 29572868]

12. Chazaud B, Inflammation and Skeletal Muscle Regeneration: Leave It to the Macrophages! *Trends Immunol*, 2020. 41(6): p. 481–492. [PubMed: 32362490]
13. Barde YA, Edgar D, and Thoenen H, Purification of a new neurotrophic factor from mammalian brain. *EMBO J*, 1982. 1(5): p. 549–53. [PubMed: 7188352]
14. Lohof AM, Ip NY, and Poo MM, Potentiation of developing neuromuscular synapses by the neurotrophins NT-3 and BDNF. *Nature*, 1993. 363(6427): p. 350–3. [PubMed: 8497318]
15. Nagahara AH and Tuszynski MH, Potential therapeutic uses of BDNF in neurological and psychiatric disorders. *Nat Rev Drug Discov*, 2011. 10(3): p. 209–19. [PubMed: 21358740]
16. Levine ES, et al. , Brain-derived neurotrophic factor rapidly enhances synaptic transmission in hippocampal neurons via postsynaptic tyrosine kinase receptors. *Proc Natl Acad Sci U S A*, 1995. 92(17): p. 8074–7. [PubMed: 7644540]
17. Kossel AH, et al. , A caged Ab reveals an immediate/instructive effect of BDNF during hippocampal synaptic potentiation. *Proc Natl Acad Sci U S A*, 2001. 98(25): p. 14702–7. [PubMed: 11724927]
18. Pedersen BK, et al. , Role of exercise-induced brain-derived neurotrophic factor production in the regulation of energy homeostasis in mammals. *Exp Physiol*, 2009. 94(12): p. 1153–60. [PubMed: 19748969]
19. Matthews VB, et al. , Brain-derived neurotrophic factor is produced by skeletal muscle cells in response to contraction and enhances fat oxidation via activation of AMP-activated protein kinase. *Diabetologia*, 2009. 52(7): p. 1409–18. [PubMed: 19387610]
20. Chan CB, et al. , Activation of muscular TrkB by its small molecular agonist 7,8-dihydroxyflavone sex-dependently regulates energy metabolism in diet-induced obese mice. *Chem Biol*, 2015. 22(3): p. 355–68. [PubMed: 25754472]
21. Clow C and Jasmin BJ, Brain-derived neurotrophic factor regulates satellite cell differentiation and skeletal muscle regeneration. *Mol Biol Cell*, 2010. 21(13): p. 2182–90. [PubMed: 20427568]
22. Barker PA, Whither proBDNF? *Nat Neurosci*, 2009. 12(2): p. 105–6. [PubMed: 19172162]
23. Hempstead BL, Brain-Derived Neurotrophic Factor: Three Ligands, Many Actions. *Trans Am Clin Climatol Assoc*, 2015. 126: p. 9–19. [PubMed: 26330656]
24. Knowles JK, et al. , Small molecule p75NTR ligand prevents cognitive deficits and neurite degeneration in an Alzheimer’s mouse model. *Neurobiol Aging*, 2013. 34(8): p. 2052–63. [PubMed: 23545424]
25. Elshaer SL, et al. , Modulation of the p75 neurotrophin receptor using LM11A-31 prevents diabetes-induced retinal vascular permeability in mice via inhibition of inflammation and the RhoA kinase pathway. *Diabetologia*, 2019. 62(8): p. 1488–1500. [PubMed: 31073629]
26. Rios M, et al. , Conditional deletion of brain-derived neurotrophic factor in the postnatal brain leads to obesity and hyperactivity. *Mol Endocrinol*, 2001. 15(10): p. 1748–57. [PubMed: 11579207]
27. Gao H, et al. , UCHL1 regulates oxidative activity in skeletal muscle. *PLoS One*, 2020. 15(11): p. e0241716. [PubMed: 33137160]
28. Gao H, et al. , UCHL1 regulates muscle fibers and mTORC1 activity in skeletal muscle. *Life Sci*, 2019. 233: p. 116699. [PubMed: 31356902]
29. Lessmann V and Brigadski T, Mechanisms, locations, and kinetics of synaptic BDNF secretion: an update. *Neurosci Res*, 2009. 65(1): p. 11–22. [PubMed: 19523993]
30. Palasz E, et al. , BDNF as a Promising Therapeutic Agent in Parkinson’s Disease. *Int J Mol Sci*, 2020. 21(3).
31. Moynagh PN, The NF-kappaB pathway. *J Cell Sci*, 2005. 118(Pt 20): p. 4589–92. [PubMed: 16219681]
32. Yang X, et al. , Muscle-generated BDNF is a sexually dimorphic myokine that controls metabolic flexibility. *Sci Signal*, 2019. 12(594).
33. Colombo E, et al. , Autocrine and immune cell-derived BDNF in human skeletal muscle: implications for myogenesis and tissue regeneration. *J Pathol*, 2013. 231(2): p. 190–8. [PubMed: 23775641]

34. Delezie J, et al. , BDNF is a mediator of glycolytic fiber-type specification in mouse skeletal muscle. *Proc Natl Acad Sci U S A*, 2019.
35. Yang J, et al. , proBDNF negatively regulates neuronal remodeling, synaptic transmission, and synaptic plasticity in hippocampus. *Cell Rep*, 2014. 7(3): p. 796–806. [PubMed: 24746813]
36. Gibon J, et al. , proBDNF and p75NTR Control Excitability and Persistent Firing of Cortical Pyramidal Neurons. *J Neurosci*, 2015. 35(26): p. 9741–53. [PubMed: 26134656]
37. Pang PT, et al. , Cleavage of proBDNF by tPA/plasmin is essential for long-term hippocampal plasticity. *Science*, 2004. 306(5695): p. 487–91. [PubMed: 15486301]
38. Woo NH, et al. , Activation of p75NTR by proBDNF facilitates hippocampal long-term depression. *Nat Neurosci*, 2005. 8(8): p. 1069–77. [PubMed: 16025106]
39. Kowianski P, et al. , BDNF: A Key Factor with Multipotent Impact on Brain Signaling and Synaptic Plasticity. *Cell Mol Neurobiol*, 2018. 38(3): p. 579–593. [PubMed: 28623429]
40. Deinhardt K and Chao MV, Shaping neurons: Long and short range effects of mature and proBDNF signalling upon neuronal structure. *Neuropharmacology*, 2014. 76 Pt C: p. 603–9. [PubMed: 23664813]
41. Mowla SJ, et al. , Biosynthesis and post-translational processing of the precursor to brain-derived neurotrophic factor. *J Biol Chem*, 2001. 276(16): p. 12660–6. [PubMed: 11152678]
42. Seidah NG, et al. , Cellular processing of the neurotrophin precursors of NT3 and BDNF by the mammalian proprotein convertases. *FEBS Lett*, 1996. 379(3): p. 247–50. [PubMed: 8603699]
43. Zhang JC, et al. , Antidepressant effects of TrkB ligands on depression-like behavior and dendritic changes in mice after inflammation. *Int J Neuropsychopharmacol*, 2014. 18(4).
44. Castets P, et al. , mTORC1 and PKB/Akt control the muscle response to denervation by regulating autophagy and HDAC4. *Nat Commun*, 2019. 10(1): p. 3187. [PubMed: 31320633]

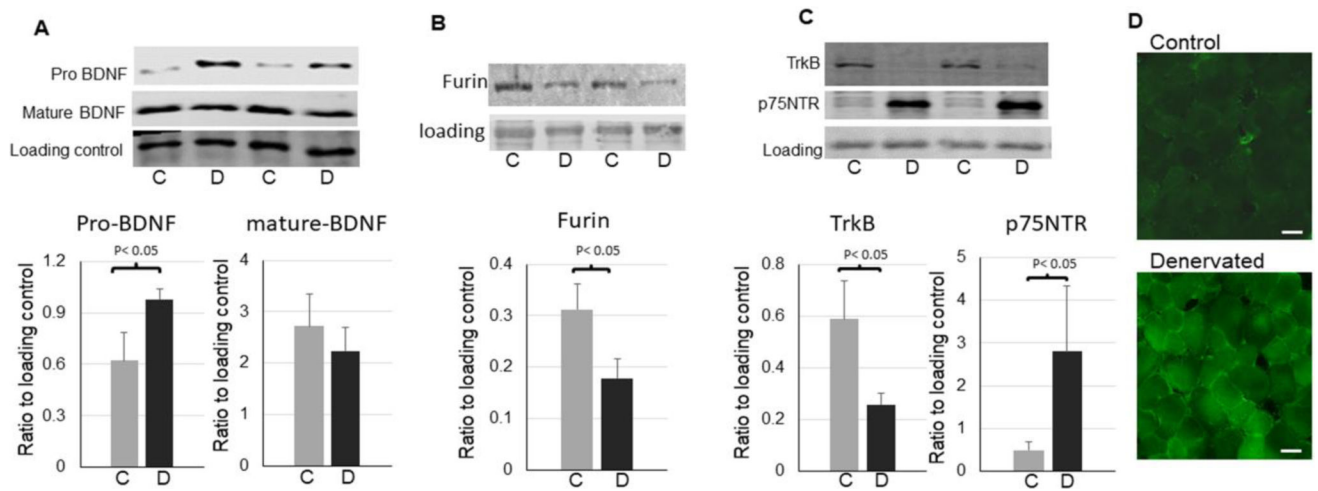


Figure 1,

Upregulation of pro-BDNF and p75NTR in denervated skeletal muscle. A: representative images and quantifications of pro-BDNF and mature BDNF in the control and denervated muscle (n=6). B: representative images and quantifications of furin in the control and denervated muscle (n=5). C: representative images and quantifications of TrkB and p75NTR in the control and denervated muscle (n=6). D: Immunofluorescent staining for p75NTR in the control and denervated muscle (scale bar = 20 μ m, 20x objective). The label “C”=control, “D”=denervated. Data is represented as means \pm S.D. analyzed by student’s t-tests.

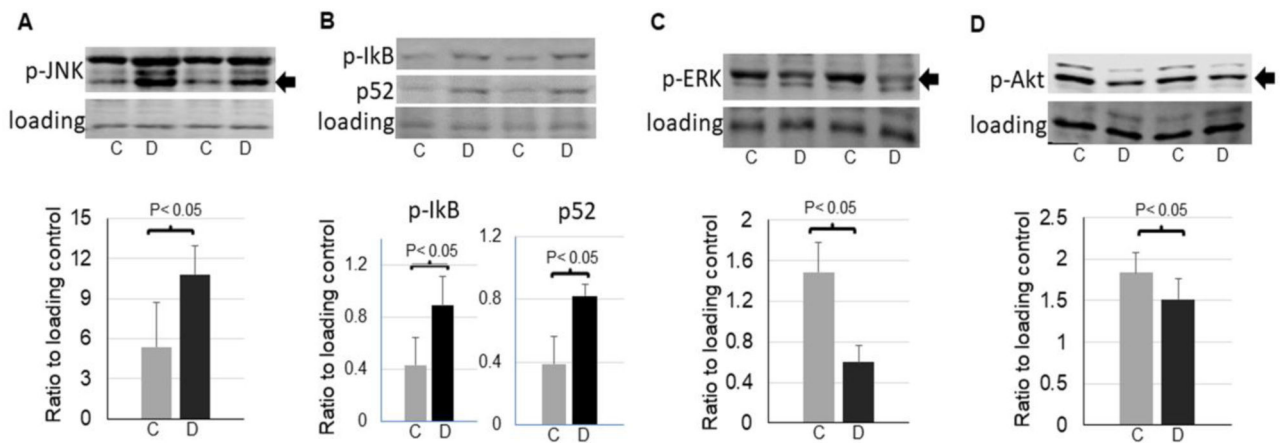


Figure 2,

Alterations of signaling pathways in the control and denervated muscle. A: representative images and quantifications of phosphorylation of JNK (54 kDa band, as indicated by an arrow) in the control and denervated muscle (n=5). B: representative images and quantifications of IκB phosphorylation and p52 in the control and denervated muscle (n=5). C: representative images and quantifications of phosphorylation of ERK (44 kDa band as indicated by an arrow) in the control and denervated muscle (n=5). D: representative images and quantifications of phosphorylation of Akt (60 kDa as indicated by an arrow) in the control and denervated muscle (n=6). Data is represented as means \pm S.D. analyzed by student's t-tests.

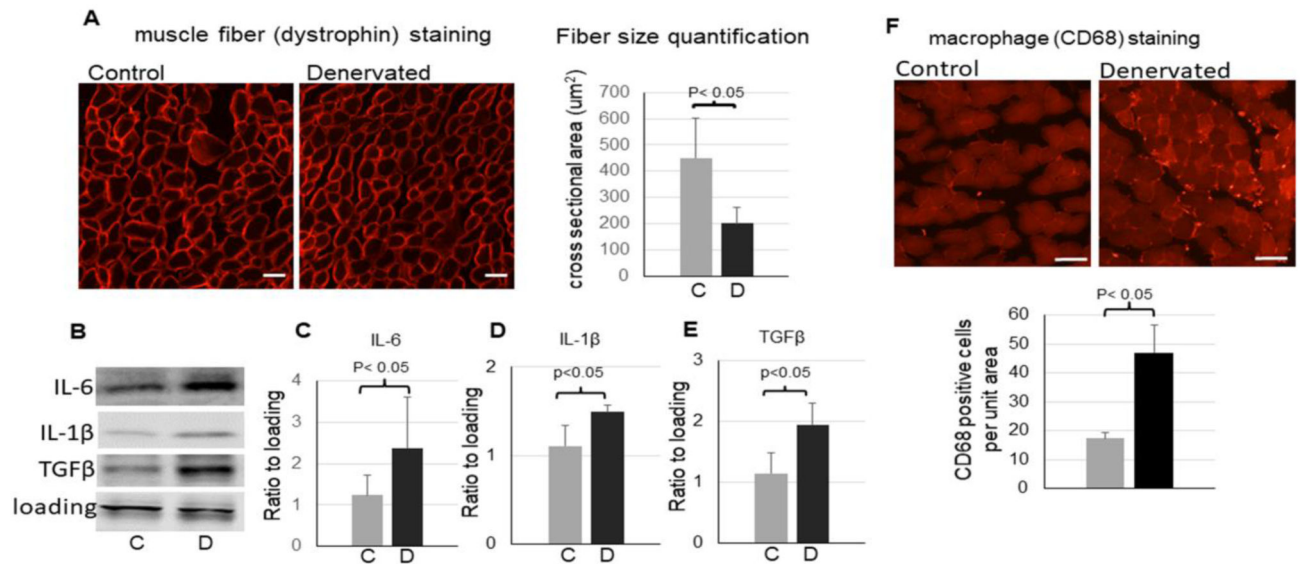


Figure 3,
Inflammation in the denervated muscle. A: representative images of dystrophin immunofluorescent staining (scale bar = 20 μm , 20x objective) and quantification (the bar graph) of muscle fiber cross sectional areas in the control and denervated muscle. B - E: representative images (B) and quantifications of IL-6 (C), IL-1 β (D), and TGF β (E) in the control and denervated muscle (n=3-4). F: representative images of immunofluorescent staining (scale bar = 50 μm , 10x objective) and quantification (bottom bar graph) of macrophage marker CD68 in the control and denervated muscle. Data is represented as means \pm S.D. analyzed by student's t-tests.

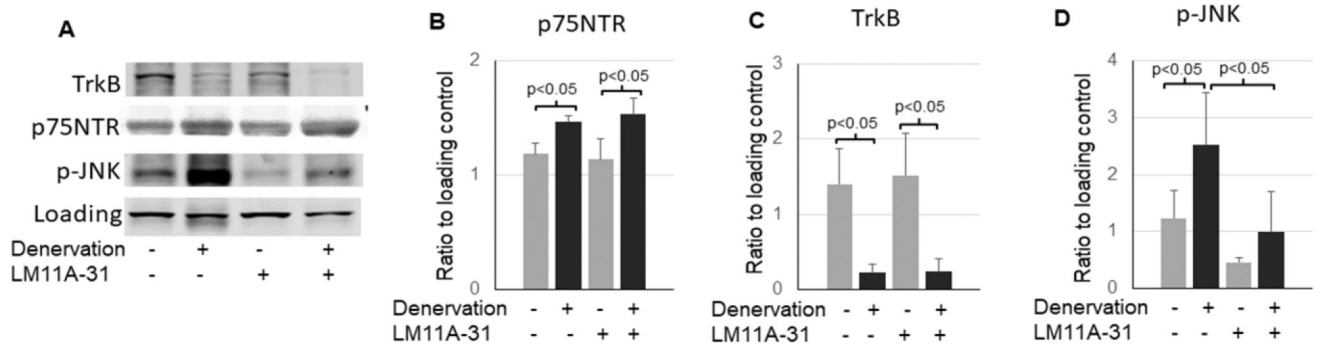


Figure 4,
Inhibition of p75NTR attenuates activation of JNK. A-D: representative of Western blot images (A) and quantifications of TrkB (B), p75NTR (C), and phosphorylation of JNK (54 kDa band) (D) in the control or denervated muscle with or without LM11A-31 treatment (n=4). Data is represented as means \pm S.D. analyzed by ANOVA analysis.

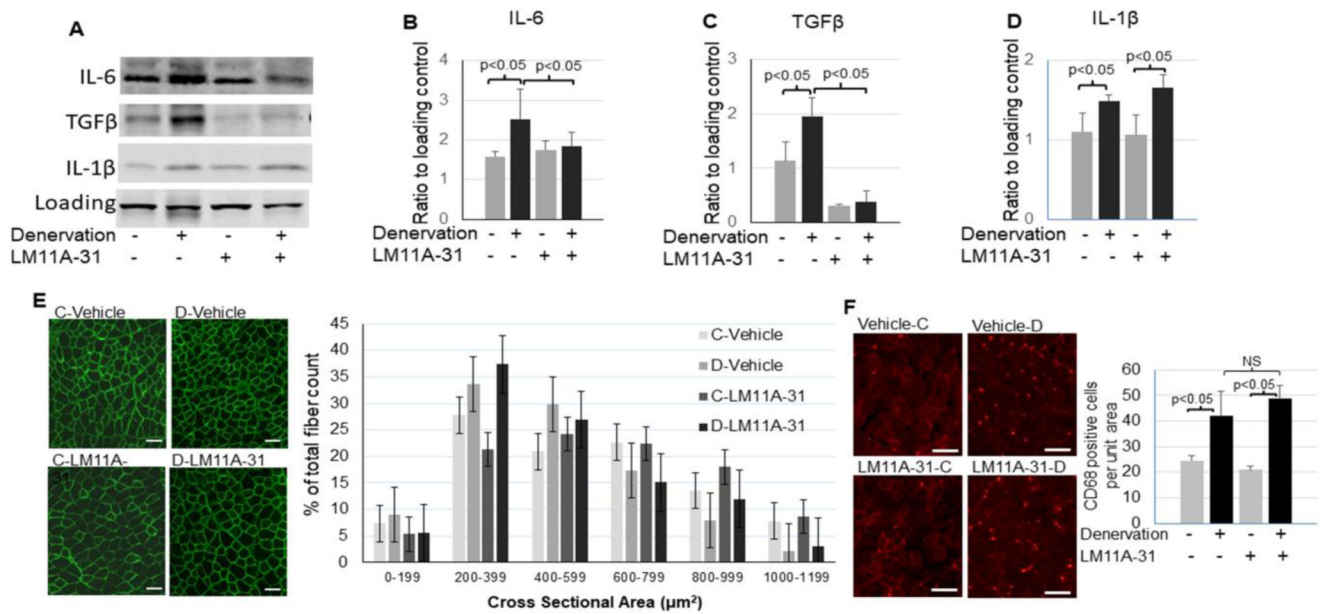


Figure 5,
 Inhibition of p75NTR reduced inflammation in denervated muscle. A – D: Representative images (A) and quantifications of IL-6 (B), TGFβ (C), and IL-1β (D) in the control or denervated muscle with or without LM11A-31 treatment (n=3–4). E: Immunofluorescent staining of dystrophin (scale bar = 50 μm, 10x objective) and quantification of muscle fiber cross sectional areas (right bar graph) of the control or denervated muscle with or without LM11A-31 treatment. F: representative images (scale bar = 50 μm, 10x objective) and quantification (right bar graph) of macrophage marker CD68 staining in the control or denervated muscle with or without LM11A-31 treatment. Data is represented as means ± S.D. analyzed by ANOVA analysis (B, C, and D). For (E) quantification, the counts were analyzed in SAS studio using a Chi Square analysis followed by comparisons between groups within each size category with a Bonferroni correction.

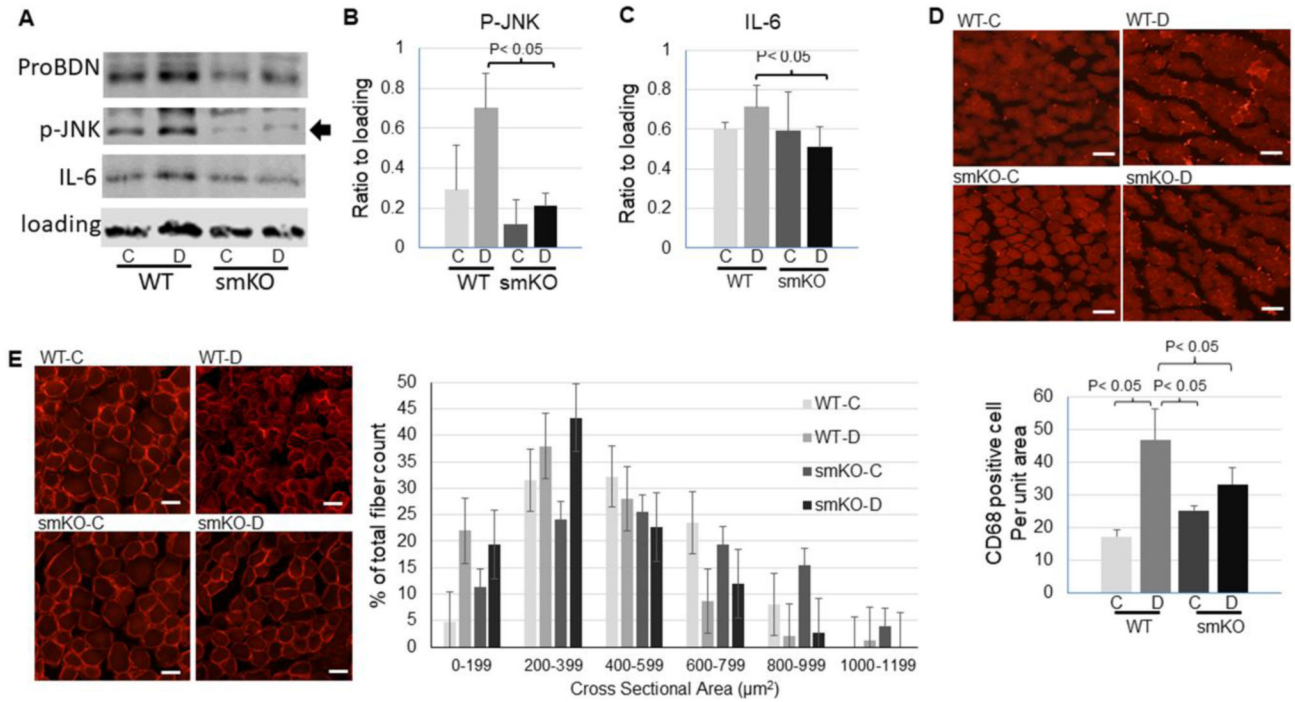


Figure 6,
 Skeletal muscle specific knockout (smKO) of BDNF attenuated inflammation in denervated muscle. A: representative images of Western blot for pro-BDNF, phosphorylation of JNK, and IL-6 in control or denervated muscle from WT or BDNF smKO mice. B-C: Quantification of phosphorylation of JNK (B) or IL-6 (C) level in control or denervated muscle from WT or BDNF smKO mice. D: representative images (scale bar = 50 µm, 10x objective) and quantification (bottom bar graph) of immunofluorescent staining of macrophage marker CD68 in control or denervated muscle from WT or BDNF smKO mice. E: Immunofluorescent staining of dystrophin (scale bar = 20 µm, 20x objective) and quantification of muscle fiber cross sectional areas (right bar graph) of the control or denervated muscle from WT or BDNF smKO mice. Data is represented as means ± S.D. analyzed by ANOVA analysis (B and C). For (E) quantification, the counts were analyzed in SAS studio using a Chi Square analysis followed by comparisons between groups within each size category with a Bonferroni correction.